JOURNAL OF CATALYSIS 125, 143–156 (1990)

Comparison between Catalytically Important Zeolites for Their Catalytic Properties and Deactivation

VASANT R. CHOUDHARY[1] AND DEEPAK B. AKOLEKAR

Chemical Engineering Division, National Chemical Laboratory, Pune 411 008, India

Received November 3, 1988; revised February 14, 1990

The catalytically important low-silica zeolites (viz., HY, CeNaY, CeNaX, and HKL) and high-silica zeolites (viz., HM, H-ZSM-5, H-ZSM-8, and H-ZSM-11) have been compared for their catalytic activity/selectivity in the cracking of cumene and isooctane and isomerization of *o*-xylene and also for their deactivation due to coke deposition in the cumene cracking. The pentasil zeolites have also been compared for their catalytic activity and shape selectivity in the conversions of methanol and ethanol to aromatics. The involvement of the strong acid sites in the cracking and isomerization reactions on the zeolites has been investigated by selectively poisoning the acid sites with pyridine. The results showed that the zeolites differ widely in their catalytic activity (per active Al and/or strong acid site), selectivity, shape selectivity, and deactivation in the catalytic reactions. The deactivation of the zeolites in cumene cracking was found to occur in the order HM > HKL > HY > CeNaY > CeNaX > H-ZSM-8 > H-ZSM-11 > H-ZSM-5.

INTRODUCTION

HY, rare earth-exchanged X- and Y-type, H-mordenite (HM), L-type, and pentasil high-silica (ZSM-5, ZSM-8 and ZSM-11) zeolites are commonly used as catalysts in various catalytic processes. These zeolites differ (*1*) very widely in their channel structures and diameters and also in their Si/Al ratios. Our earlier studies (*2, 3*) of the acidity distributions of the HY, CeNaY, CeNaX, HKL, HM, H-ZSM-5, H-ZSM-8, and H-ZSM-11 zeolites have indicated that these zeolites differ widely in acidity distribution and number of strong acid sites compared to their Al content. The changes in the acidity of zeolites are directly reflected in their catalytic activity and selectivity. It is, therefore, very interesting to compare these zeolites for their catalytic properties and also for their deactivation due to coke deposition. For a direct comparison, it is necessary to carry out a particular measurement on the zeolites under identical conditions. However, the literature on such zeolite studies is scarce.

In the present investigation, the above zeolites have been compared for their catalytic properties and deactivation due to coke deposition by carrying out cumene cracking, isooctane cracking, *o*-xylene isomerization, and methanol and ethanol conversion reactions over the zeolites in a pulse microreactor.

EXPERIMENTAL

The HY, CeNaY, CeNaX, HKL, HM, H-ZSM-5, H-ZSM-8, and H-ZSM-11 zeolites and their properties are given in Table 1. The zeolite HM (Zeolon 900 H, in the form of 20- to 50-mesh aggregates) was obtained from Norton Co. (U.S.A.). The HKL zeolite was prepared by exchanging KL (Laposil 200 series, obtained from Laporte, UK) with 0.1 *M* HCL. The zeolite HY was obtained by deammoniating NH_4Y (Si/Al = 2.4 and Na/Al = 0.08) packed in a stainless-steel tube (o.d. 6 mm; zeolite bed, 4-mm diameter × 10 mm long) in a flow of

[1] To whom all correspondence should be addressed.

0021-9517/90 $3.00

TABLE 1

Zeolites and Their Properties

Zeolite	Si/Al	Degree of H^+ or Ce^{+3} exchange	N_2 sorption capacity (mmol · g^{-1})	Average crystal size (μm)	Crystal shape	Strong acid sites (mmol · g^{-1})
HY	2.42	0.92	—	<1	Spheroidal	0.78
CeNaY	2.42	0.72	8.6	<1	Spheroidal	0.44
CeNaX	1.26	0.90	7.5	≈2	Irregular	0.51
HKL	3.0	0.95	4.2	≈1	Irregular	0.22
HM	6.60	0.97	—	<1	Spheroidal	0.77
H-ZSM-5	31.1	0.99	5.0	≈4	Polyhedral	0.25
H-ZSM-8	29.6	0.96	4.9	≈4	Cubical	0.31
H-ZSM-11	35.3	1.00	6.4	≈2	Ovate	0.07

nitrogen (10 $cm^3 \cdot min^{-1}$) at 623 K for 4 h. The H-ZSM-5 zeolite was obtained by deammoniating NH_4-ZSM-5 (Si/Al = 31.1, Na/Al = 0.01) at 773 K in a flow of nitrogen (10 $cm^3 \cdot min^{-1}$) for 4 h. The H-ZSM-11 zeolite was obtained by calcining in air the NH_4 · TBA-ZSM-11 (Si/Al = 35.3) at 773 K for 12 h. The preparation and characterization of the NH_4Y (*4*), NH_4-ZSM-5 (*5, 6*), NH_4 · TBA-ZSM-11 (*3*), and H-ZSM-8 (*7*) zeolites have been given earlier. The CeNaY and CeNaX zeolites were provided by Professor J. Weitkamp (University of Stuttgart, FRG). The preparation and characterization of the Ce-exchanged zeolites have been described elsewhere (*8*).

All the zeolites were pressed binder-free and crushed to particles of 0.2–0.3 mm size. Before using them, the zeolies CeNaY, CeNaX, HY, HKL, and HM were calcined *in situ* at 623 K for 4 h in a flow of nitrogen (10 $cm^3 \cdot min^{-1}$) passing through the zeolite bed. The *in situ* calcination of the pentasil zeolite was done at 673 K in a flow of nitrogen (10 $cm^3 \cdot min^{-1}$) for 1 h. In the calcination of all the zeolites, the temperature was raised at a rate of 10 K min^{-1}. The N_2 sorption capacity (measured at p/p_s = 0.3 and 78 K by dynamic adsorption/desorption technique) and the crystal size and morphology (examined by SEM) of the zeolites are given in Table 1. All the zeolites (Table 1) have already been compared for their acidity and acid strength distribution in our earlier paper (*2*). The pretreatment conditions for the zeolites used for measuring their acidity and catalytic properties were the same.

The catalytic activity and selectivity of the zeolites in the cumene and isooctane cracking, *o*-xylene isomerization, and methanol and ethanol-to-aromatics conversion reactions have been determined in a pulse microreactor (4.0 mm i.d.) connected to a gas chromatograph (Perkin–Elmer Sigma 3B gas chromatograph with a flame ionization detector) using nitrogen as a carrier gas. The details of the microreactor and the experimental procedures for measuring the catalytic activity have been given earlier (*5, 7*).

The activity and selectivity of the strong acid sites (measured in terms of the chemisorption of pyridine at 623 K) of the zeolites were determined by poisoning the strong acid sites with pyridine chemisorbed at 623 K and carrying out the activity/selectivity measurements on the poisoned zeolite. A detailed procedure for selectively poisoning strong acid sites of the zeolites has been given earlier (*4, 5, 9*). Reproducibility of results on the zeolites (with or without poi-

TABLE 2

Comparison of the Catalytic Activity of the Zeolites in the Cumene Cracking at 600 K

Zeolite	Conversion of cumene (%)			N_{Al} (molecules per Al* per s)	N_s (molecules per SA per s)
	On unpoisoned zeolite (i.e., on all acid sites)	On poisoned zeolite (i.e., on weak acid sites)	On strong acid sites		
HY	84.3	19.4	64.9	69.6	226.8
CeNaY	67.3	39.7	27.6	81.2	188.8
CeNaX	75.6	64.8	10.8	52.4	67.2
HKL	14.2	6.6	7.6	11.2	95.5
HM	38.0	3.4	34.6	54.4	122.4
H-ZSM-5	11.4	0.5	10.9	62.3	118.6
H-ZSM-8	34.0	3.4	30.6	174.4	267.6
H-ZSM-11	4.13	1.14	3.0	24.8	114.0

Note. Amount of catalyst, 50 mg; N_2 flow rate, 1 $dm^3 \cdot min^{-1}$; pulse size, 8.0 μl; pressure, 270 kPa.

soning) was checked by repeating the experiments. The results were reproducible within about 5%.

For comparing the deactivation characteristics of the zeolites, a number of pulses of cumene were passed over the zeolites one after the other at 1-h intervals at 600 K. After the injection of the last pulse, the methanol-to-aromatics conversion on the pentasil zeolites was carried out. The deactivated zeolites (except the X, Y, and L zeolites) were then heated at 773 K in a flow of oxygen-free nitrogen (100 $cm^3 \cdot min^{-1}$) for 1 h and their activity in the cumene cracking was measured at 600 K.

RESULTS AND DISCUSSION

Catalytic Activity/Selectivity

The data on the catalytic activity of the zeolites in the cumene cracking, isooctane cracking, and *o*-xylene isomerization reactions over the zeolites are compared in Tables 2, 3, and 4, respectively. The product distribution, xylene loss, and *p*-xylene/*m*-xylene ratio in the *o*-xylene isomerization over the zeolites with and without poisoning by pryidine are presented in Tables 5–7. The comparison of the data on the formation of aromatics and their distribution in the methanol and ethanol conversion reactions over the pentasil zeolites is given in Tables 8 and 9. The zeolites have been arranged in order of their turnover rates in the above reactions, as shown in Table 10.

In order to determine separately the catalytic activity of the weak and strong acid sites of the zeolites, the cumene cracking, isooctane cracking, and *o*-xylene isomerization reactions were carried out on the zeolite with and without blocking (or poisoning) of their strong acid sites with pyridine chemisorbed at 623 K. In the present case, strong and weak acid sites are defined as follows: Strong acid sites are those which can chemisorb pyridine at and above 623 K, whereas all other acid sites (i.e., those sites which can chemisorb pyridine only at <623 K) are considered weak acid sites. In the present study, the chemisorption is defined as the amount of base retained on the presaturated zeolite after it was swept with pure nitrogen for a period of 1 h.

The catalytic activity of the zeolites in the cracking and isomerization reactions, apart from the conversion of reactant (or the formation of aromatics in the alcohol conversion reactions), is also expressed in

TABLE 3

Comparison of the Catalytic Activity of the Zeolites in the Isooctane Cracking at 573 K

Zeolite	Conversion of isooctane (%)			N_{Al} (molecules per Al* per s)	N_s (molecules per SA per s)
	On unpoisoned zeolite (i.e., on all acid sites)	On poisoned zeolite (i.e., on weak acid sites)	On strong acid sites		
HY	55.1	2.9	52.2	0.29	1.18
CeNaY	81.1	1.1	80.0	0.63	3.10
CeNaX	97.7	1.0	96.7	0.44	3.40
HKL	9.9	2.9	7.0	0.10	1.15
HM	98.1	0.0	98.1	0.90	2.20
H-ZSM-5	0.3 0.5[a]	—	—	—	—
H-ZSM-8	0.3 0.6[a]	—	—	—	—
H-ZSM-11	0.4 0.9[a]	—	—	—	—

Note. Amount of catalyst, 100 mg; N_2 flow rate, 60 $cm^3 \cdot min^{-1}$; pressure, 200 kPa; pulse size, 3.2 μl.
[a] At 673 K.

terms of the catalytic turnover rates, N_{Al} and N_s, indicating the average activity of the tetrahedral Al atom and of the strong acid site of the zeolite [N_{Al} indicates catalytic turnover rate per active Al (i.e., number of molecules reacted per active Al per second); N_s indicates catalytic turnover rate per strong acid site (i.e., number of molecules reacted per strong acid sites per second)]. The catalytic activity of the pen-

TABLE 4

Comparison of the Catalytic Activities of the Zeolites in the *o*-Xylene Isomerization at 600 K

Zeolite	Conversion of *o*-xylene (%)			N_{Al} (molecules per Al* per s)	N_s (molecules per SA per s)
	On unpoisoned zeolite (i.e., on all acid sites)	On poisoned zeolite (i.e., on weak acid sites)	On strong acid sites		
HY	34.8	8.0	26.8	6.8	22.0
CeNaY	46.0	14.4	31.6	13.2	46.4
CeNaX	57.7	37.7	20.0	9.6	25.2
HKL	16.7	10.6	6.1	3.1	17.4
HM	77.4	1.0	76.4	26.4	64.4
H-ZSM-5	1.7	0.4	1.3	2.4	3.3
H-ZSM-8	7.1	1.0	6.1	8.0	12.6
H-ZSM-11	0.9	0.2	0.7	1.2	6.4

Note. Amount of catalyst, 50 mg; N_2 flow rate, 440 $cm^3 \cdot min^{-1}$; pressure, 245 kPa; pulse size, 3.4 μl.

TABLE 5

Product Distribution in the *o*-Xylene Isomerization on the Low-Silica Zeolites with and without Poisoning

Zeolites	HY		CeNaY		CeNaX		HKL	
	Unpoisoned	Poisoned	Unpoisoned	Poisoned	Unpoisoned	Poisoned	Unpoisoned	Poisoned
Conversion (%)	34.80	8.00	46.00	14.40	57.70	37.70	16.70	10.60
Product distribution [hydrocarbons (wt%)]								
Aliphatics	0.03	—	—	—	0.11	—	0.1	0.3
Benzene	—	—	0.50	—	1.24	0.54	0.8	0.7
Toluene	4.96	1.55	14.10	5.24	17.60	12.20	4.4	2.7
p-Xylene	6.06	1.40	2.80	1.09	5.55	3.86	1.3	1.2
m-Xylene	19.30	3.42	17.60	3.20	22.10	12.00	6.8	4.4
o-xylene	65.20	92.00	54.00	85.00	42.30	62.30	83.3	89.4
C_{9+}-aromatics	4.45	1.63	11.00	4.87	11.10	9.10	3.3	1.3
Total	100	100	100	100	100	100	100	100

tasil zeolites in the alcohol-to-aromatics conversion reactions is expressed in terms of the formation of aromatics (i.e., wt% of aromatics in the hydrocarbons formed) and also in terms of the catalytic turnover rates per active Al (n_{Al}) and per strong acid site (n_s). The active Al (or Al*) is defined as the framework Al which is not blocked by Na^+ cation. The turnover numbers (N and n) refer to unpoisoned catalyst.

Cracking of cumene. The results of the cumene cracking on the zeolites (Table 2) indicate the following:

Among the zeolites, the turnover rate per Al* (N_{Al}) is highest for the H-ZSM-8 zeolite, whereas, the turnover rate per strong acid site (N_s) is also highest for the H-ZSM-8 zeolite.

The cumene cracking activity of the poisoned zeolites is very appreciable. This indicates the involvement of weak acid sites of the zeolites in the cumene cracking. The activity of the poisoned zeolites in the cumene cracking can, therefore, be considered as a measure of their active weak acid sites. The zeolites can be arranged in the order of their weak acid sites which are active in the cumene cracking, as follows:

CeNaX > CeNaY > HY > HKL > HM > H-ZSM-8 > H-ZSM-11 > H-ZSM-5.

(The above order is obtained by comparing the results on the poisoned zeolites.) Also, it is possible to obtain a rough estimate of the relative concentrations of the strong

TABLE 6

Distribution of Hydrocarbons in the *o*-Xylene Isomerization in the High-Silica Zeolites with and without Poisoning

Zeolites	H-ZSM-5		H-ZSM-8		H-ZSM-11		HM	
	Unpoisoned	Poisoned	Unpoisoned	Poisoned	Unpoisoned	Poisoned	Unpoisoned	Poisoned
Conversion (%)	1.70	0.40	7.10	1.00	0.90	0.21	77.40	1.00
Product distribution [hydrocarbons (wt%)]								
Aliphatics	0.01	—	0.01	—	0.02	0.01	0.30	—
Benzene	—	—	—	—	—	—	2.10	—
Toluene	0.02	—	0.11	0.05	0.14	—	19.30	0.11
p-Xylene	0.74	0.20	3.38	0.50	0.33	0.11	9.80	0.32
m-Xylene	0.93	0.20	2.92	0.40	0.41	0.09	25.10	0.57
o-xylene	98.30	99.60	92.90	99.00	99.10	99.79	22.60	99.00
C_{9+}-aromatics	—	—	0.60	0.05	—	—	20.80	—
Total	100	100	100	100	100	100	100	100

TABLE 7

Data on the Xylene Loss, Xylene Selectivity, and *p*-X/*m*-X Ratio in the *o*-Xylene Isomerization over the Unpoisoned and Pyridine-Poisoned Zeolites

Zeolite	Xylene loss (wt%)		Selectivity for *p*- and *m*-xylenes (%)		*p*-X/*m*-X ratio	
	Unpoisoned	Poisoned	Unpoisoned	Poisoned	Unpoisoned	Poisoned
HY	9.4	3.2	72.9	60.3	0.3	0.4
CeNaY	25.6	10.1	44.3	30.5	0.2	0.3
CeNaX	30.1	21.8	47.9	42.1	0.2	0.3
HKL	8.6	5.0	48.5	52.8	0.2	0.3
HM	42.5	—	45.1	57.0	0.4	0.5
H-ZSM-5	0.03	—	96.0	100.0	0.8	1.0
H-ZSM-8	0.50	—	88.7	90.0	0.7	1.3
H-ZSM-11	0.20	—	82.2	95.2	0.8	1.2

and the weak acid sites on the zeolites by comparing the cumene cracking activity of the strong acid sites of the zeolite with that of the poisoned one. The results (Table 2) reveal that the concentration of the weak acid sites relative to that of the strong acid sites is somewhat higher for the CeNaX and CeNaY but lower for the other zeolites. This is in agreement with the acidity distribution on the zeolites (*2*).

Isooctane cracking. Comparison of the catalytic activity of the zeolites with and without poisoning in the isooctane cracking (Table 3) reveals the following facts.

TABLE 8

Data on the Extent of Aromatization and Distribution of Aromatics in the Methanol and Ethanol Conversion Reactions over the Pentasil Zeolites

Reaction:	Methanol conversion			Ethanol conversion		
Zeolite:	H-ZSM-5	H-ZSM-8	H-ZSM-11	H-ZSM-5	H-ZSM-8	H-ZSM-11
Conversion of alcohol (%)	100	100	100	100	100	100
Concentration of aromatics in the hydrocarbons (wt%)	19.30	33.10	1.09	20.50	30.70	0.79
Distribution of aromatics (wt%)						
Benzene	7.03	11.10	10.09	10.48	15.11	10.13
Toluene	36.29	34.14	25.69	42.02	42.02	25.32
Ethyl benzene	0.84	1.42	4.59	3.20	0.36	3.80
p-Xylene	17.24	13.35	10.05	11.92	13.03	11.39
m-Xylene	19.10	25.83	14.74	14.97	19.61	15.19
o-Xylene	7.80	8.31	9.17	5.41	6.45	8.86
(Total xylenes)	(44.14)	(47.49)	(34.86)	(32.3)	(39.09)	(35.44)
C_{9+}-aromatics	11.70	5.89	24.77	12.00	3.42	25.31
Total	100	100	100	100	100	100
p-X/(*m*- and *o*-X)	0.64	0.39	0.42	0.58	0.50	0.47

Note. Amount of catalyst, 0.1 g; N_2 flow rate, 25 $cm^3 \cdot min^{-1}$; pulse size, 2.5 μl; temperature, 648 K, pressure 185 kPa.

TABLE 9

Comparison of the Catalytic Activity of the Pentasil Zeolites in the Conversions of Methanol and Ethanol to Aromatics at 648 K

Zeolite	Methanol conversion			Ethanol conversion		
	Aromatic Rate of formation $n(\mu g \cdot s^{-1})$	$n_{Al} \times 10^{18}$ (μg per s per Al*)	$n_s \times 10^{18}$ (μg per s per SA)	Aromatic Rate of formation $n(\mu g \cdot s^{-1})$	$n_{Al} \times 10^{18}$ (μg per s per Al*)	$n_s \times 10^{18}$ (μg per s per SA)
H-ZSM-5	783	26.0	51.8	1916	63.6	126.8
H-ZSM-8	1343	42.1	7.19	2870	89.9	153.7
H-ZSM-11	44	1.7	10.5	74	2.9	17.7

The isooctane cracking activity of the pentasil zeolites is extremely poor because of the fact that the isooctane molecules [because of their bulkier size (critical molecular size: 0.70 nm)] cannot penetrate the channels of the zeolites and the reaction occurs only on the external surface of the zeolite crystallites.

The very low catalytic activity of the poisoned HY, CeNaY, CeNaX, HKL, and HM zeolites indicates that the isooctane cracking occurs essentially on the strong acid sites. This is consistant with earlier observations for the HY, CeNaY, and HM zeolites (*4*).

Among the HY, CeNaY, CeNaX, HKL, and HM zeolites, the turnover rate per Al* is highest for the HM, whereas the turnover

TABLE 10

Ordering of the Zeolites according to Acidity and Catalytic Activity in Different Reactions

	Zeolite order
Strong acid sites	HY ≃ HM > CeNaX > CeNaY > H-ZSM-8 > H-ZSM-5 > HKL > H-ZSM-11
Turnover rate per active Al	
Cumene cracking	H-ZSM-8 > CeNaY > HY > H-ZSM-5 > HM > CeNaX > H-ZSM-11 > HKL
Isooctane cracking	HM > CeNaY > CeNaX > HY > HKL
o-Xylene isomerization	HM > CeNaY > CeNaX > H-ZSM-8 > HY > HKL > H-ZSM-5 > H-ZSM-11
Methanol-to-aromatics conversion	H-ZSM-8 > H-ZSM-5 > H-ZSM-11
Ethanol-to-aromatic conversion	H-ZSM-8 > H-ZSM-5 > H-ZSM-11
Turnover rate per strong acid site	
Cumene cracking	H-ZSM-8 > HY > CeNaY > HM > H-ZSM-5 > H-ZSM-11 > HKL > CeNaX
Isooctane cracking	CeNaX > CeNaY > HM > HY > HKL
o-Xylene isomerization	HM > CeNaY > CeNaX > HY > HKL > H-ZSM-8 > H-ZSM-11 > H-ZSM-5
Methanol-to-aromatics conversion	H-ZSM-8 > H-ZSM-5 ≫ H-ZSM-11
Ethanol-to-aromatics conversion	H-ZSM-8 > H-ZSM-5 ≫ H-ZSM-11

rate per strong acid site is highest for the CeNaX zeolite. However, the turnover rates are lowest for the HKL zeolite.

o-Xylene isomerization. The results of the conversion of *o*-xylene on the zeolites with and without poisoning (Table 4) indicate that the reaction of *o*-xylene occurs also on the weak acid sites, particularly those of the X, Y, and L zeolites. The isomerization activity of the zeolites is in the order

$$\text{HM} > \text{CeNaX} > \text{CeNaY} > \text{HY} > \text{HKL} > \text{H-ZSM-8} > \text{H-ZSM-5} > \text{H-ZSM-11}.$$

The turnover numbers, N_{Al} and N_s, for the reaction are also highest for the HM and lowest for the H-ZSM-11 zeolite. The turnover numbers (N_{Al} and N_s) for the pentasil zeolites (which have narrow pores) are much lower than those for the other zeolites (which have large pores). This is most probably due to the fact that, because of the larger size of *o*-xylene, its reaction on the pentasil zeolites is influenced severely by the intracrystalline mass transfer.

The product distribution in the *o*-xylene isomerization (Tables 5–7) varied from zeolite to zeolite and was also strongly influenced by the poisoning. Poisoning of the zeolites results in a decrease in xylene loss and an increase in paraselectivity of the zeolites; the increase in paraselectivity is particularly very significant in the case of the pentasil zeolites, mostly due to the increase in the diffusional resistance in the zeolites.

The xylene loss (which reflects on the selectivity for isomerization in the conversion of *o*-xylene) for the zeolites (Table 7) varies drastically from zeolite to zeolite. The zeolites differ greatly from each other in their selectivity for isomerization and also for formation of *p*-xylene (or paraselectivity). They can be arranged in order of isomerization and paraselectivity as follows:

$$\text{H-ZSM-5} > \text{H-ZSM-8} > \text{H-ZSM-11} > \text{HY} > \text{HKL} > \text{CeNaX} > \text{HM} > \text{CeNaY};$$

for the para-selectivity,

$$\text{H-ZSM-5} \simeq \text{H-ZSM-11} > \text{H-ZSM-8} > \text{HM} > \text{HY} > \text{CeNaY} > \text{CeNaX} > \text{HKL}.$$

Alcohol-to-aromatics conversion. The formation of aromatics at 648 K in the conversion of methanol and ethanol on pentasil zeolites poisoned with pyridine irreversibly chemisorbed at 673 K has been found to be negligibly small. This is consistent with earlier observations (*6, 9*) that aromatization in the alcohol conversion process over H-ZSM-5 and H-ZSM-8 occurs only on the strong acid sites.

In both the alcohol conversions, the aromatization activity [i.e., the rate of formation of aromatics (n) and also the rates of aromatics formation per active Al (n_{Al}) or per strong acid sites (n_s)] of the pentasil zeolite (Table 9) is in the order

$$\text{H-ZSM-8} > \text{H-ZSM-5} \gg \text{H-ZSM-11}.$$

This indicates that the aromatization activity possessed by the framework Al or by the strong acid sites depends on the structure of the pentasil zeolite; it is highest for the H-ZSM-8 and lowest for the H-ZSM-11 zeolite.

The product distribution in both the alcohol-to-aromatics conversions (Table 8) reveals that the distribution of the aromatics formed on the pentasil zeolites is quite different. The H-ZSM-5 shows paraselectivity higher than that of the H-ZSM-8 and H-ZSM-11 zeolites. The formation of C_{9+}-aromatics (higher aromatics/polyalkylbenzenes containing nine or more carbon atoms per molecule) in both the alcohol conversions is highest on the H-ZSM-11 and lowest on the H-ZSM-8 zeolite. However, for the formation of C_6–C_8 aromatics, the above order is reversed. In methanol conversion, Derouane *et al.* (*10*) and Harrison *et al.* (*11, 12*) have also observed higher production of C_{9+}-aromatics over ZSM-11 than over ZSM-5, which has been attributed to a decreased degree of pore con-

straint and the presence of cavities in ZSM-11 larger than those in ZSM-5. Apart from these two reasons (which are based on the differences in the channel structure and the volume of cavities at the channel intersections of the two zeolites), the large difference in the acidity of the pentasil zeolites (Table 1) (*2*) is also expected to be responsible for the different distributions of aromatics obtained over the pentasil zeolites.

The acidity of pentasil zeolite can influence the distribution of aromatics through secondary alkylation/dealkylation reactions as follows. On H-ZSM-11, because of its much lower acidity, alkylation of the lower aromatics is favored over dealkylation of the higher aromatics, thus increasing the concentration of the latter. On the H-ZSM-8 and H-ZSM-5 zeolites, the aromatics are dealkylated on the large number of strong acid sites available on the zeolites, reducing the concentration of the higher aromatics. Influence of secondary aromatic conversion reactions (viz., alkylation, dealkylation, isomerization, and disproportionation) on the distribution of aromatics formed in both methanol and ethanol conversion on H-ZSM-5 has been indicated in earlier studies (*13–16*). It seems that there exists a relationship between the acidity (strong acid sites) of the pentasil zeolites and the formation of higher aromatics on the zeolites; the latter decreases the former increases. It may be noted that the order of the formation of higher aromatics on the pentasil zeolites is exactly opposite that of their strong acid sites. This is also supported by the earlier observation that the concentration of higher aromatics is decreased with the increase in the strong acid sites in both methanol and ethanol conversions on H-ZSM-5 (with different Si/Al ratios and degrees of H^+-exchange and also pretreated at different conditions (*6, 13, 14*).

In the case of the H-ZSM-5 and H-ZSM-8 zeolites, the lower paraselectivity observed over H-ZSM-8 indicates a small but significant difference in the channel structure of the two zeolites. However, the lower concentration of C_{9+}-aromatics obtained over H-ZSM-8 is mostly due to its higher acidity (i.e., the presence of a large number of strong acid sites).

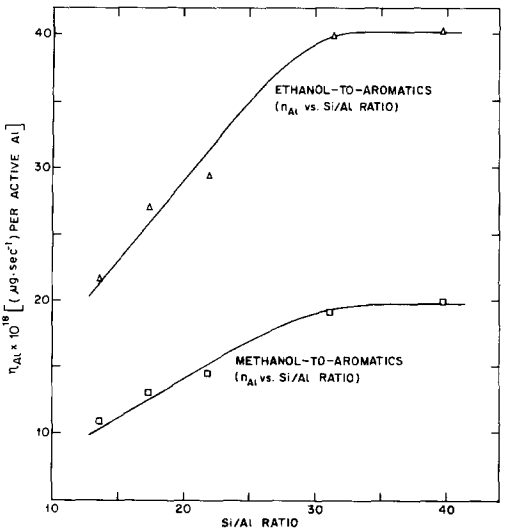

FIG. 1. Variation in the rate of formation of aromatics per Al* (n_{Al}) in the conversions of methanol and ethanol over H-ZSM-5 with its Si/Al ratio. [The data were recalculated from the data given by Choudhary and Nayak (*13*).]

The dependence of the catalytic turnover rates (expressed as the amount of aromatics formed per second per active Al) for the formation of aromatics in methanol and ethanol conversions over H-ZSM-5 on its Si/Al ratio is shown in Fig. 1. A similar trend has been observed for the dependence of the strong acid sites per active Al (*2*) and also of the active acid sites per Al (*17*) of H-ZSM-5 on its Si/Al ratio. The data on the aromatization activity were recalculated from the data obtained earlier by Choudhary and Nayak (*13*).

Deactivation of Zeolites in Cumene Cracking

In order to compare the zeolites for their deactivation due to coke deposition, the cumene cracking activity of the zeolites was measured as a function of pulse number. The dependence of the conversion of cu-

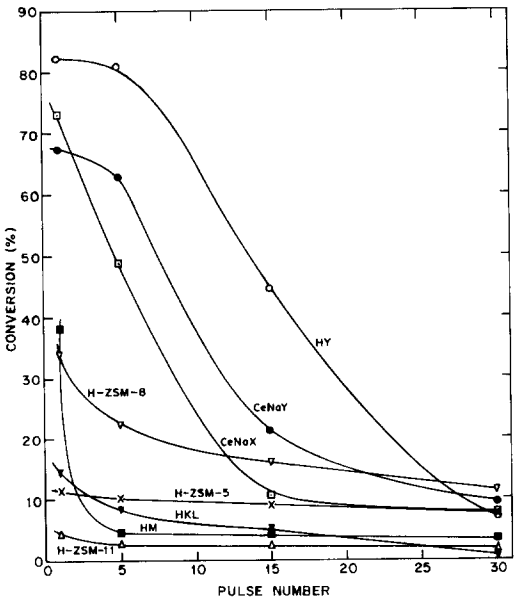

FIG. 2. Dependence of the cumene cracking activity (i.e., conversion of cumene) of the different zeolites on the pulse number. Amount of zeolite, 50 mg; N_2 flow rate, 1.0 $dm^3 \cdot min^{-1}$; pulse size, 8.0 μl; temperature, 600 K.

mene on the pulse number for the different zeolites is shown in Fig. 2. For comparing the deactivation trends of the zeolites, the data showing the influence of pulse number on the fractional cumene cracking activity [x = (conversion of cumene for a particular pulse)/(conversion of cumene for the first pulse)] of the zeolites are represented in Fig. 3.

A comparison of the data in Fig. 3 reveals that the rate of catalyst deactivation in the cumene cracking is highest for the HM and lowest for the H-ZSM-5 zeolite. For the 30th pulse, the fractional catalytic activity (x) shown by the zeolites is in the order

H-ZSM-5 > H-ZSM-11
> H-ZSM-8 > CeNaX
> CeNaY > HKL > HY ≃ HM.

However, the rate of deactivation of the zeolites was in the order

HM > HKL > HY > CeNaY
> CeNaX > H-ZSM-8
> H-ZSM-11 > H-ZSM-5.

In the earlier studies, the deactivation of ZSM-5-type zeolites was also found to be much slower than that of the large-pore zeolites, such as Y zeolite in hydrocarbon conversion reactions (*18, 19*), HL or HY (*20*) and HM (*21*) in methanol-to-hydrocarbons conversions, and X or Y (*22*) in alkylation of benzene with ethylene and ethanol. In conversion of methanol or ethanol to aromatics, the deactivation of H-ZSM-8 was faster than that of H-ZSM-5 (*7, 15, 16*). All these earlier observations are consistent with the present ones.

The concentration of aromatics in the hydrocarbons formed in the methanol conversion on the deactivated H-ZSM-5 and H-ZSM-8 zeolites (i.e., the zeolites after

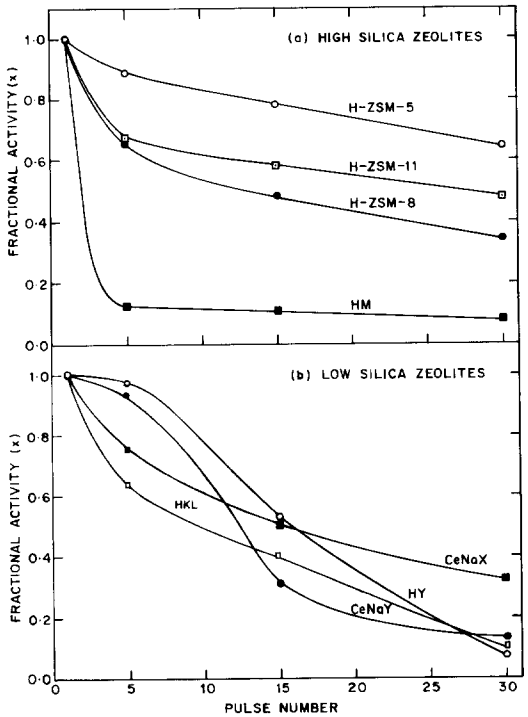

FIG. 3. Effect of pulse number on the fractional catalytic activity (x) of the zeolite in the cracking of cumene at 600 K.

injection of the 30th cumene pulse) at 648 K was found to be 18.5 and 25.8%, respectively. Thus, the relative decrease in the catalytic activity of the zeolites for the aromatization in the methanol conversion is much less than that for the cracking of cumene. From this observation, it is inferred that the deactivation of the strong acid sites of the pentasil zeolites in the cumene pulse experiments occurs only to a small extent, and the observed large decrease in the cumene cracking activity of the zeolites with the increase in the pulse number (Fig. 3a) is mostly a result of the increased diffusional resistance for cumene in the zeolite channels. Since the diffusional resistance for methanol in the zeolites is expected to be much smaller than that for cumene, their aromatization activity is affected to a relatively smaller extent.

Further, when the deactivated H-ZSM-5, H-ZSM-8, and H-ZSM-11 zeolites were heated at 773 K in the flow of an inert gas (oxygen-free nitrogen) for 1 h, their cumene-cracking activity was regained to a large extent; their activity (x) was increased from 0.64 to 0.87 for H-ZSM-5, 0.34 to 0.82 for H-ZSM-8, and 0.48 to 0.85 for H-ZSM-11. The partial gain in catalytic activity of the pentasil zeolites reveals that their deactivation observed for the cumene cracking (Fig. 3) is partly due to blockage of some of the zeolite channels by strongly sorbed or occluded large hydrocarbon molecules (formed simultaneously during the cumene cracking), which are cracked to small fragments at higher temperatures and diffuse out from the zeolite channels. The gradual blockage of the zeolite channels (inside and near pore openings) and deposition of coke on the external surface of zeolite crystallites are expected to result in a gradual increase in the intracrystalline diffusional resistance in the zeolites, which is mostly responsible for the decreased activity for the cumene cracking. The fact that the catalytic activity is not fully regained indicates that some of the strong acid sites (mostly very strong ones) are deactivated by deposition of carbonaceous residue on them. The deposition of coke on the external surface of the zeolite crystallites may also affect the catalytic activity in the cumene cracking to a small extent because of the deactivation of external acid sites.

The loss of the aromatization activity due to the cumene pulse experiments on the H-ZSM-5 and H-ZSM-8 zeolites is expected to be due to the blockage and/or deactivation of some of the strong acid sites on the zeolites and is also due to some extent to coke deposition on the external surface of the zeolite crystallites, which causes blockage of some of the pore openings. Deposition of coke (i.e., polynuclear aromatics) in the zeolite channels is, however, not favored because of restricted transition-state molecular shape-selectivity of the ZSM-5 zeolite (*21, 23*) and the same is expected to be true for the ZSM-8 and ZSM-11 zeolites.

The sharp decrease in the cumene cracking activity of the HM (which is a large-pore zeolite having a unidimensional pore system) with the pulse number is due mostly to coke deposition at the entrance of its unidimensional pores (i.e., due to pore mouth blockage), which makes the inner active sites of the zeolite unavailabe for the catalytic reaction. The heating of the deactivated HM at elevated temperatures (i.e., at 773 K) in the inert atmosphere has not resulted in a significant increase in its activity. This indicates that the coke on the zeolite is mostly in the form of polynuclear aromatics.

The decrease in the cumene cracking activity for HY, CeNaY, and CeNaX (which are large-pore zeolites having three-dimensional pore systems) with the pulse number is expected to be due to the deactivation of the active acid sites of the zeolites by coke deposition and is also due to some extent to pore mouth blockage of the zeolites by coke deposition resulting in an increase in the mass transfer resistance.

Deactivation of the zeolites due to coking is expected to depend on their acidity, shape selectivity, and mass transfer proper-

ties and, consequently, on the factors (viz., Si/Al ratio, degree of cation exchange, pretreatment conditions, poisoning, deposition of foreign material in zeolite channels or on the external surface of zeolite crystallites, crystal size, particle size, crystal aggregates, etc.) affecting these properties. Therefore, changes in these properties may lead to a change in the observed order of the zeolites for their deactivation due to coking. However, because of spatial constraints acting on reactions responsible for the formation of carbonaceous residue, the medium-pore zeolites (ZSM-5, ZSM-8, and ZSM-11) are expected to be deactivated at slower rates compared to those of the large pore (X, Y, and M) zeolites. Also, the zeolites having unidimensional channel systems are expected to be deactivated at faster rates than those having two- or three-dimensional channel systems.

Comparison between the Pentasil Zeolites

For comparing the pentasil zeolites for their sorption, acidity, and catalytic properties, the zeolites having somewhat similar Si/Al ratios and degrees of H^+-exchange are used. The crystal size of H-ZSM-11 is, however, smaller than that of the H-ZSM-5 and H-ZSM-8 zeolites. Because of the smaller crystal size of the H-ZSM-11 and also the presence of less channel constraint (as both the intersecting channels in ZSM-11 are linear), the intracrystalline diffusional resistance in H-ZSM-11 is expected to be much smaller than that in the other two zeolites.

The N_2 sorption capacities (Table 1) of the H-ZSM-5 and H-ZSM-8 zeolites are more or less similar, whereas the sorption capacity for H-ZSM-11 is significantly higher than that for the H-ZSM-5 and H-ZSM-8 zeolites. The higher sorption capacity of H-ZSM-11 is attributed to the greater volume of cavities at the channel intersection of the ZSM-11 zeolites (*10*).

The pentasil zeolites show the following order of acidity (i.e., the strong acid sites) and catalytic activity in the cumene cracking, *o*-xylene isomerization, and alcohol (methanol and ethanol)-to-aromatics conversion reactions:

$$\text{H-ZSM-8} > \text{H-ZSM-5} \gg \text{H-ZSM-11}.$$

The above order remains the same even when the acidity is expressed as the number of strong acid sites produced per structural active Al and also when the catalytic activity is expressed in terms of the turnover rates per structural active Al. It may be noted that the observed lower catalytic activity of the H-ZSM-11 is only because of its lower acidity and is certainly not due to mass transfer limitation, as the diffusional resistance in H-ZSM-11 is expected to be much less pronounced than that in the H-ZSM-5 and H-ZSM-8 zeolites.

In the catalytic reactions over the three pentasil zeolites, the turnover rates per strong acid site (N_s and n_s) for the H-ZSM-8 zeolite were found to be the highest. The aromatization in the alcohol conversions over the pentasil zeolites occurs only on the strong acid sites. The pentasil zeolites show the following order for their turnover rates per strong acid sites (n_s) in both the alcohol-to-aromatics conversion reactions:

$$\text{H-ZSM-8} > \text{H-ZSM-5} \gg \text{H-ZSM-11}.$$

This indicates that the aromatization activity of the strong acid sites in the pentasil zeolites varies from zeolite to zeolite to a very large extent. The observed large difference in the catalytic activity of the strong acid sites of the pentasil zeolites is expected to be due to the difference in the acid strength distribution of the strong acid sites of the zeolites. This leads to the conclusion that the average strength of the strong acid sites on the zeolites is highest for H-ZSM-8 and lowest for H-ZSM-11. Thus, the pentasil zeolites follow the same order for both number and strength of strong acid sites present in them.

The large difference in number and strength of strong acid sites present on the pentasil zeolites (with somewhat similar Si/Al ratios) reveals that the acidity produced

by the framework Al^- anions in the zeolites depends strongly on the structure of the zeolite.

In the methanol- and ethanol-to-aromatics conversions, ZSM-5 shows higher para-selectivity than those of ZSM-8 and ZSM-11 and the formation of higher aromatics (C_{9+}-aromatics) is highest over the ZSM-11 and lowest over the ZSM-8 zeolite.

The fact that H-ZSM-5 and H-ZSM-8 show a large difference in acidity, catalytic activity, and shape selectivity (as discussed above) indicates that the two zeolites differ significantly in structure.

In the cumene cracking, the deactivation of the pentasil zeolites occurs in the order

$$\text{H-ZSM-8} > \text{H-ZSM-11} > \text{H-ZSM-5}.$$

The deactivation of H-ZSM-8 in methanol- and ethanol-to-aromatics conversions was also found to be higher than that of H-ZSM-5 (*7*).

CONCLUSIONS

The zeolites differ widely in their catalytic properties and deactivation due to coke deposition. The catalytic activities per active framework Al^- or per strong acid site for the zeolites differing in structure and also for the zeolites (e.g., H-ZSM-5) having the same structure but differing in Si/Al ratios (up to a certain Si/Al ratio) are not the same and depend strongly on both the structure and the topology of the zeolite and the chemical environment of the framework Al^-.

Among the pentasil zeolites, the ZSM-8 zeolite possesses the highest acidity (i.e., higher strength acid sites) and catalytic activity, whereas ZSM-11 possesses the lowest acidity and catalytic activity. The catalyst deactivation in the cumene cracking is, however, highest for the ZSM-8 and lowest for the ZSM-5 zeolite. In the alcohol-to-aromatics conversions, the formation of C_{9+}-aromatics is highest over the ZSM-11 and lowest over the ZSM-8 zeolite. The channel structure of ZSM-8 is expected to be significantly different from that of the other two pentasil zeolites.

In the cumene cracking process, the deactivation of HY, CeNaY, and CeNaX zeolites is due to coke deposition in the zeolite channels and to pore mouth blockage, and that of HM and HKL zeolites is due mostly to pore mouth blockage. However, in the case of the H-ZSM-5, H-ZSM-8, and H-ZSM-11 zeolites, their deactivation is due to the blockage of some of the zeolite channels by strongly sorbed or occluded large hydrocarbon molecules and the deposition of coke on the external surface of the zeolite crystallites, both causing a large increase in the mass transfer resistance for bulkier reactant molecules in the zeolite channels.

ACKNOWLEDGMENT

The authors are grateful to Professor J. Weitkamp (Technische Chemie-I, University of Stuttgart, FRG) for providing the CeNaY and CeNaX zeolite samples.

REFERENCES

1. Breck, D. W., "Zeolite Molecular Sieves." Wiley, New York, 1974.
2. Choudhary, V. R., and Akolekar, D. B., *J. Catal.* **119,** 525 (1989).
3. Akolekar, D. B., "Sorption, Diffusion and Catalytic Reactions on Zeolites and Zeolite-like Materials, Ph.D. thesis, University of Poona, Poona, 1987.
4. Choudhary, V. R., *Zeolites* **7,** 272 (1987).
5. Nayak, V. S., and Choudhary, V. R., *Appl. Catal.* **4,** 333 (1982).
6. Nayak, V. S., and Choudhary, V. R., *J. Catal.* **81,** 26 (1983).
7. Akolekar, D. B., and Choudhary, V. R., *J. Catal.* **105,** 416 (1987).
8. Choudhary, V. R., Srinivasan, K. R., and Akolekar, D. B., *Zeolites* **9,** 115 (1989).
9. Nayak, V. S., and Choudhary, V. R., *Appl. Catal.* **9,** 251 (1984).
10. Derouane, E. G., Dejaifve, P., Gabelica, Z., and Vedrine, J. C., *Discuss. Faraday Soc.* **72,** 331 (1981).
11. Harrison, I. D., Leach, H. F., and Whan, D. A., *in* "Proceedings, 6th Int. Zeolite Conf., Reno, USA" (D. H. Olson and A. Bisio, Eds.), p. 479. 1983.
12. Harrison, I. D., Leach, F. H., and Whan, D. A., *Zeolites* **7,** 21 (1987).

13. Choudhary, V. R., and Nayak, V. S., *Zeolites* **5,** 325 (1985).
14. Nayak, V. S., and Choudhary, V. R., *Appl. Catal.* **10,** 137 (1984).
15. Choudhary, V. R., and Sansare, S. D., *Indian J. Technol.* **23,** 326 (1983).
16. Choudhary, V. R., and Sansare, S. D., *Appl. Catal.* **10,** 147 (1984).
17. Choudhary, V. R., and Nayak, V. S., *Acta Phys. Chem.* **31**(1, 2), 167 (1985).
18. Rollman, L. D., *J. Catal.* **47,** 113 (1977).
19. Rollman, L. D., and Walsh, D. E., *J. Catal.* **56,** 139 (1979).
20. Langner, B. E., *Appl. Catal.* **2,** 289 (1982).
21. Dejaifve, P., Auroux, A., Gravelle, P. C., Vedrine, J. C., Gabelica, Z., and Derouane, E. G., *J. Catal.* **70,** 123 (1981).
22. Chandawar, K. H., Kulkarni, S. B., and Ratnasamy, P., *Appl. Catal.* **4,** 287 (1982).
23. Derouane, E. G., *in* "Catalysis by Acids and Bases" (B. Imelik *et al.*, Eds.), p. 221. Elsevier, Amsterdam, 1985.